Journal of Solid State Chemistry 185 (2012) 1–9

Contents lists available at SciVerse ScienceDirect

Journal of Solid State Chemistry

journal homepage: www.elsevier.com/locate/jssc

The new high-pressure borate $Co_7B_{24}O_{42}(OH)_2 \cdot 2\,H_2O$—Formation of edge-sharing BO_4 tetrahedra in a hydrated borate

Stephanie C. Neumair [a], Reinhard Kaindl [1,b], Hubert Huppertz [a,*]

[a] Institut für Allgemeine, Anorganische und Theoretische Chemie, Leopold-Franzens-Universität Innsbruck, Innrain 52a, A-6020 Innsbruck, Austria
[b] Institut für Mineralogie und Petrographie, Leopold-Franzens-Universität Innsbruck, Innrain 52f, A-6020 Innsbruck, Austria

ARTICLE INFO

Article history:
Received 18 July 2011
Received in revised form
10 October 2011
Accepted 17 October 2011
Available online 25 October 2011

Keywords:
High-pressure chemistry
Multianvil
Structure elucidation
Borates

ABSTRACT

The new borate hydrate $Co_7B_{24}O_{42}(OH)_2 \cdot 2\,H_2O$ was synthesized under high-pressure/high-temperature conditions of 6 GPa and 880 °C in a Walker-type multianvil apparatus. The compound crystallizes in the orthorhombic space group *Pbam* ($Z=2$) with the lattice parameters $a=819.0(2)$, $b=2016.9(4)$, $c=769.9(2)$ pm, $V=1.2717(4)$ nm^3, $R_1=0.0758$, $wR_2=0.0836$ (all data). The new structure type of $Co_7B_{24}O_{42}(OH)_2 \cdot 2\,H_2O$ is built up from corner-sharing BO_4 tetrahedra forming corrugated layers, that are interconnected among each other by two edge-sharing BO_4 tetrahedra (B_2O_6 units) forming Z-shaped channels. Interestingly, the here presented structure of $Co_7B_{24}O_{42}(OH)_2 \cdot 2\,H_2O$ is closely related to the structures of $M_6B_{22}O_{39} \cdot H_2O$ (M=Fe, Co), which exhibit BO_4 tetrahedra in an intermediate state on the way to edge-sharing BO_4 tetrahedra.

1. Introduction

The research on borates with the multianvil high-pressure technique [1] provides various opportunities to open up new fields of synthesis in solid state chemistry. Apart from the transformation of known borates into new high-pressure polymorphs (*e.g.* δ-BiB_3O_6 [2]), the syntheses of new compounds with unexpected structural features emphasized the prominence of this method (*e.g.* β-SnB_4O_7 [3], $RE_3B_5O_{12}$ (RE=Sc [4], Er–Lu [5])). The most striking discovery in our research was the structural motif of edge-sharing BO_4 tetrahedra (B_2O_6 unit), which was observed first in the compounds $RE_4B_6O_{15}$ (RE=Dy, Ho) [6,7] and later on in the rare-earth borates α-$RE_2B_4O_9$ (RE=Sm–Ho) [8–10]. In these examples, only a fraction of one-third ($RE_4B_6O_{15}$ (RE=Dy, Ho)) or one-tenth (α-$RE_2B_4O_9$ (RE=Sm–Ho)) of the BO_4 tetrahedra shares a common edge with a second tetrahedron. With the synthesis of HP–MB_2O_4 (M=Co, Ni) [11,12] and β-FeB_2O_4 [13], it was possible to synthesize three isotypic borates, in which every BO_4 tetrahedron bridges to a second one *via* a common edge. In 2010, Jin et al. found the structural feature of edge-sharing BO_4 tetrahedra in the compound $KZnB_3O_6$, synthesized under ambient pressure conditions [14,15]. Recently, we were able to synthesize a fifth structure type with B_2O_6 units in the field of alkali metal borates: HP–KB_3O_5, being the first compound, which exhibits all three possible conjunctions of the main structural elements in borates simultaneously: corner-sharing BO_3 groups, corner-sharing BO_4 units, and edge-sharing BO_4 tetrahedra in one structure type [16]. As up to now it is not possible to predict the occurrence of the B_2O_6 units, we are interested in the detailed formation conditions of edge-sharing BO_4 tetrahedra. In 2010, we characterized the new compounds $M_6B_{22}O_{39} \cdot H_2O$ (M=Fe, Co) [17], which show the structural feature of a BO_4 tetrahedron and a BO_3 group, that can be regarded as an intermediate state on the way to edge-sharing BO_4 tetrahedra. The here presented compound $Co_7B_{24}O_{42}(OH)_2 \cdot 2\,H_2O$ is closely related to the structures of $M_6B_{22}O_{39} \cdot H_2O$ (M=Fe, Co) but exhibits truly edge-sharing BO_4 tetrahedra. We report the synthesis, structural details, and properties of the new high-pressure cobalt borate hydrate $Co_7B_{24}O_{42}(OH)_2 \cdot 2\,H_2O$.

2. Experimental section

2.1. Synthesis

The new borate hydrate $Co_7B_{24}O_{42}(OH)_2 \cdot 2\,H_2O$ was synthesized under high-pressure/high-temperature conditions of 6 GPa and 880 °C, starting from Co_3O_4 and H_3BO_3 (Eq. (1)).

$$7\,Co_3O_4 + 72\,H_3BO_3 \xrightarrow{6\,GPa,\ 880\,^\circ C} 3\,Co_7B_{24}O_{42}(OH)_2 \cdot 2\,H_2O + 99\,H_2O + 3.5\,O_2 \quad (1)$$

A stoichiometric mixture of Co_3O_4 (Merck KGaA, Darmstadt, Germany, p.a.) and H_3BO_3 (Merck KGaA, Darmstadt, Germany, 99.5%) was ground together and filled into a boron nitride

* Corresponding author. Fax: +435125072934.
E-mail address: hubert.huppertz@uibk.ac.at (H. Huppertz).
[1] Present address: Joanneum Research Forschungsgesellschaft mbH, Materials—Institute for Surface Technologies and Photonic Functional Surfaces, Leobner Strasse 94, A-8712 Niklasdorf, Austria.

0022-4596/$ - see front matter © 2011 Elsevier Inc. All rights reserved.
doi:10.1016/j.jssc.2011.10.028

crucible (Henze BNP GmbH, HeBoSint® S100, Kempten, Germany). The crucible was placed inside of an 18/11-assembly, which was compressed by eight tungsten carbide cubes (Ceratizit, Reutte, Austria). A detailed description of the assembly preparation can be found in Refs. [1,18–21]. The assembly was compressed and heated in a multianvil device based on a Walker-type module and a 1000 t press (both devices from the company Voggenreiter, Mainleus, Germany). In detail, the sample was compressed up to 6 GPa in 3 h, then heated to 880 °C in 10 min and kept there for 5 min. Afterwards, the sample was cooled down to 400 °C in 15 min and cooled down to room temperature by switching off the heating. After a decompression period of 9 h, the recovered MgO-octahedron (pressure transmitting medium, Ceramic Substrates & Components Ltd., Newport, Isle of Wight, UK) was broken apart and the sample carefully separated from the surrounding boron nitride crucible. The new compound $Co_7B_{24}O_{42}(OH)_2 \cdot 2\,H_2O$ was gained in the form of violet, air- and water-resistant crystals. Higher temperatures as well as longer heating periods during the synthesis led to $Co_6B_{22}O_{39} \cdot H_2O$ and another yet unknown phase.

2.2. Crystal structure analysis

The powder diffraction pattern of $Co_7B_{24}O_{42}(OH)_2 \cdot 2\,H_2O$ was obtained in transmission geometry from flat samples of the reaction product, using a STOE STADI P powder diffractometer with Mo$K\alpha_1$ radiation (Ge monochromator, $\lambda = 70.93$ pm). The diffraction pattern showed reflections of $Co_7B_{24}O_{42}(OH)_2 \cdot 2\,H_2O$ and reflections of at least one by-product of the synthesis. The experimental powder pattern tallies well with the theoretical patterns simulated from single-crystal data. By indexing the reflections of the cobalt borate hydrate with Treor [22–24], we derived the lattice parameters $a = 819.3(3)$, $b = 2016.3(5)$, and $c = 769.8(2)$ pm, and a unit-cell volume of 1.2717(4) nm^3. This confirmed the lattice parameters, received from the single-crystal X-ray diffraction study (Table 1).

Small single crystals of the cobalt borate hydrate $Co_7B_{24}O_{42}(OH)_2 \cdot 2\,H_2O$ could be isolated by mechanical fragmentation. The single crystal intensity data of $Co_7B_{24}O_{42}(OH)_2 \cdot 2\,H_2O$ were collected at room temperature using a Nonius Kappa-CCD diffractometer with graphite-monochromatized Mo$K\alpha$ radiation ($\lambda = 71.073$ pm). A semiempirical absorption correction based on equivalent and redundant intensities (Scalepack [25]), was applied to the intensity data. All relevant details of the data collection and evaluation are listed in Table 1.

According to the systematic extinctions, the orthorhombic space group *Pbam* was derived. The structure solution and parameter refinement (full-matrix least-squares against F^2) were performed using the Shelx-97 software suite [26,27] with anisotropic atomic displacement parameters for all atoms. The positional parameters of the refinements and interatomic distances are listed in Tables 2 and 3. Additional details of the crystal structure investigations may be obtained from the Fachinformationszentrum Karlsruhe (crysdata@fiz-karlsruhe.de, http://www.fiz-informationsdienste.de/en/DB/icsd/depotanforderung.html), D-76344 Eggenstein-Leopoldshafen (Germany) on quoting the Registry No. CSD-422991.

2.3. IR spectroscopy

FTIR absorption spectra of the crystals were recorded on a BaF_2 plate in transmission with a Bruker Vertex 70 FT-IR spectrometer

Table 1
Crystal data and structure refinement of $Co_7B_{24}O_{42}(OH)_2 \cdot 2\,H_2O$ (standard deviations in parentheses).

Empirical formula	$Co_7B_{24}O_{42}(OH)_2 \cdot 2\,H_2O$
Molar mass (g mol^{-1})	1414.00
Crystal system	Orthorhombic
Space group	*Pbam*
Powder data	
Powder diffractometer	STOE Stadi P
Radiation	Mo$K\alpha_1$ ($\lambda = 70.93$ pm)
a (pm)	819.3(3)
b (pm)	2016.3(5)
c (pm)	769.8(2)
V (nm^3)	1.2717(4)
Single crystal data	
Single crystal diffractometer	Enraf–Nonius Kappa CCD
Radiation	Mo$K\alpha$ ($\lambda = 71.073$ pm)
a (pm)	819.0(2)
b (pm)	2016.9(4)
c (pm)	769.9(2)
V (nm^3)	1.2717(4)
Formula units per cell	2
Calculated density (g cm^{-3})	3.693
Crystal size (mm^3)	$0.08 \times 0.03 \times 0.03$
Temperature (K)	293(2)
Absorption coefficient (mm^{-1})	4.675
F(000)	1366
θ range (deg.)	2.0–35.0
Range in hkl	± 13, ± 32, $-12/+11$
Total no. of reflections	17310
Independent reflections	2967 ($R_{int} = 0.0949$)
Reflections with $I \geq 2\sigma(I)$	2230 ($R_\sigma = 0.0577$)
Data/parameters	2967/199
Absorption correction	multi-scan (Scalepack [25])
Goodness-of-fit on F_i^2	1.067
Final R indices [$I \geq 2\sigma(I)$]	$R_1 = 0.0454$
	$wR_2 = 0.0757$
R indices (all data)	$R_1 = 0.0758$
	$wR_2 = 0.0836$
Largest diff. peak and hole (e Å^{-3})	0.89/−1.22

(resolution ~0.5 cm^{-1}), attached to a Hyperion 3000 microscope in a spectral range from 550 to 7500 cm^{-1}. 64 scans of sample and background were acquired. The spectra were corrected for atmospheric influences, using the OPUS 6.5 software. Background correction and peak fitting followed *via* polynomial and folded Gaussian–Lorentzian functions. Absorption bands around 2800 cm^{-1} result from contamination by nail polish from the single crystal X-ray diffraction experiment.

2.4. Raman spectroscopy

Confocal Raman spectra of single crystals were obtained with a HORIBA JOBIN YVON LabRam-HR 800 Raman micro-spectrometer. The sample was excited by the 532 nm emission line of a 30 mW Nd-YAG-laser under an OLYMPUS 100× objective (N.A.=0.9). The size and power of the laser spot on the surface were approximately 1 μm and 0.5 mW. The scattered light was dispersed by a grating with 1800 lines/mm and collected by a 1024 × 256 open electrode CCD detector. The spectral resolution, determined by measuring the Rayleigh line, was about 1.4 cm^{-1}. Third order polynomial and convoluted Gauss–Lorentz functions were applied for background correction and band fitting. The wavenumber accuracy of about 0.5 cm^{-1} was achieved by adjusting the zero-order position of the grating and regularly checked by a Neon spectral calibration lamp.

Table 2
Atomic coordinates and equivalent isotropic displacement parameters U_{eq} (Å^2) of $Co_7B_{24}O_{42}(OH)_2 \cdot 2\,H_2O$ (space group *Pbam*). U_{eq} is defined as one third of the trace of the orthogonalized U_{ij} tensor (standard deviations in parentheses).

Atom	Wyckoff-Position	x	y	z	U_{eq}
Co1	4*h*	0.30695(6)	0.43302(2)	½	0.0087(2)
Co2	4*h*	0.40029(6)	0.17280(2)	½	0.0070(2)
Co3	4*g*	0.09526(6)	0.38153(2)	0	0.0111(2)
Co4	2*a*	0	0	0	0.0087(2)
O1	8*i*	0.0219(2)	0.07205(8)	0.1924(2)	0.0069(3)
O2	8*i*	0.0227(2)	0.44681(9)	0.1794(2)	0.0096(3)
O3	8*i*	0.0373(2)	0.19021(8)	0.1711(2)	0.0061(3)
O4	8*i*	0.0572(2)	0.29613(8)	0.3043(2)	0.0069(3)
O5	8*i*	0.2515(2)	0.13178(8)	0.3105(2)	0.0067(3)
O6	8*i*	0.2564(2)	0.01237(8)	0.3116(2)	0.0082(3)
O7	8*i*	0.3000(2)	0.24172(8)	0.1951(2)	0.0060(3)
O8	8*i*	0.3054(2)	0.35801(8)	0.3052(2)	0.0069(3)
O9	4*h*	0.0489(3)	0.4126(2)	½	0.0114(5)
H1	8*i*	0.016(6)	0.429(2)	0.407(6)	0.06(2)
O10	4*h*	0.0654(3)	0.0686(2)	½	0.0073(4)
O11	4*h*	0.2747(3)	0.2644(2)	½	0.0073(5)
O12	4*g*	0.0220(3)	0.2885(2)	0	0.0057(4)
O13	4*g*	0.2590(3)	0.1475(2)	0	0.0064(4)
H2	4*g*	0.25(2)	0.108(4)	0	0.08(3)
O14	4*g*	0.2849(3)	0.0150(2)	0	0.0097(5)
O15	4*g*	0.3382(3)	0.3721(2)	0	0.0069(5)
B1	8*i*	0.1483(3)	0.0702(2)	0.3323(3)	0.0068(5)
B2	8*i*	0.2132(3)	0.1766(2)	0.1763(3)	0.0068(5)
B3	8*i*	0.2324(3)	0.2929(2)	0.3341(3)	0.0069(5)
B4	8*i*	0.3702(4)	0.0075(2)	0.1683(4)	0.0091(5)
B5	8*i*	0.4213(3)	0.3697(2)	0.1683(3)	0.0071(5)
B6	8*i*	0.4816(3)	0.2402(2)	0.1669(3)	0.0070(5)

3. Results and discussion

3.1. Crystal structure of $Co_7B_{24}O_{42}(OH)_2 \cdot 2\,H_2O$

Figs. 1 and 2 give a view of the centrosymmetric crystal structure of $Co_7B_{24}O_{42}(OH)_2 \cdot 2\,H_2O$ along [001] and [0$\bar{1}$0], respectively. The borate is built up from corrugated layers, composed of corner-sharing BO_4 tetrahedra. The layers are interconnected to a network structure *via* two edge-sharing BO_4 tetrahedra ($[B_2O_6]^{6-}$ unit), generating Z-shaped channels, in which the cations are arranged. Fig. 3 shows that two B_2O_6 units are connected to "vierer" rings [28] *via* corner-sharing: a new connectivity of $[B_2O_6]^{6-}$ units observed here for the first time.

From the 15 crystallographically independent oxygen atoms in this structure, O3 and O7 are bridging three BO_4 tetrahedra simultaneously ($O^{[3]}$), while all other oxygen atoms link two BO_4 tetrahedra. A differentiation between the differently coordinated oxygen atoms is depicted in Fig. 1 ($O^{[2]}$: dark corners of polyhedra and small dark spheres, $O^{[3]}$: light corners of polyhedra).

The B–O bond-lengths for B1–B6 in $Co_7B_{24}O_{42}(OH)_2 \cdot 2\,H_2O$ vary between 140.7 and 158.7 pm with an average B–O bond-length of 148.0 pm. This corresponds with the known average value of 147.6 pm for BO_4 tetrahedra [29,30]. Fig. 3 shows the interatomic distances inside the two linked B_2O_6 units (edge-sharing BO_4 tetrahedra). As expected, the B–O distances inside the B_2O_2 ring (B4–O2: 150.9(3), 155.4(4) pm) are longer than the average value for four-coordinated boron atoms (147.6 pm) [29,30]. Inside the B_2O_6 unit, the B···B distance comes to 214.8(5) pm, which is higher than the values found in most other borates with edge-sharing BO_4 tetrahedra, *e.g.* $Dy_4B_6O_{15}$ (207.2(8) pm) [6], α-$Sm_2B_4O_9$ (207.1(9) pm) [10], β-FeB_2O_4 (208.3(5) pm) [13], and $KZnB_3O_6$ (207.9(4) pm) [14,15]. A comparison of the distances inside the B_2O_6 units of all known compounds with edge-sharing BO_4 tetrahedra is depicted in Fig. 4. The only compound exhibiting higher B···B distances for edge-sharing BO_4 tetrahedra is HP-KB_3O_5 [16], which comprises a three-fold coordinated oxygen ion ($O^{[3]}$) at the common edge of the BO_4 tetrahedra, leading to enhanced distances inside of the B_2O_2 ring and therewith to a remarkably

Table 3
Interatomic distances (pm) in $Co_7B_{24}O_{42}(OH)_2 \cdot 2\,H_2O$ (space group *Pbam*), calculated with the single-crystal lattice parameters.

Co1–O10		211.7(3)	Co2–O5	2×	207.3(2)	Co3–O12		196.9(2)
Co1–O8	2×	213.0(2)	Co2–O4	2×	207.7(2)	Co3–O2	2×	199.9(2)
Co1–O9		215.3(3)	Co2–O9		210.9(3)	Co3–O15		199.9(3)
Co1–O6	2×	222.1(2)	Co2–O11		211.4(2)			
		Ø=216.2			**Ø=208.7**			**Ø=199.2**
Co4–O1	4×	208.3(2)						
Co4–O14	2×	235.3(3)						
		Ø=217.3						
B1–O1		149.4(3)	B2–O3		146.8(3)	B3–O4		145.5(3)
B1–O5		151.1(3)	B2–O5		140.7(3)	B3–O7		158.7(3)
B1–O6		147.3(3)	B2–O7		150.1(3)	B3–O8		146.0(3)
B1–O10		145.9(3)	B2–O13		152.5(3)	B3–O11		144.3(3)
		Ø=148.4			**Ø=147.5**			**Ø=148.6**
B4–O2		150.9(3)	B5–O1		144.7(3)	B6–O3		147.6(3)
B4–O2		155.4(3)	B5–O3		153.7(3)	B6–O4		142.8(3)
B4–O6		144.8(3)	B5–O8		143.7(3)	B6–O7		150.3(3)
B4–O14		147.9(3)	B5–O15		146.4(3)	B6–O12		144.8(3)
		Ø=149.8			**Ø=147.1**			**Ø=146.4**

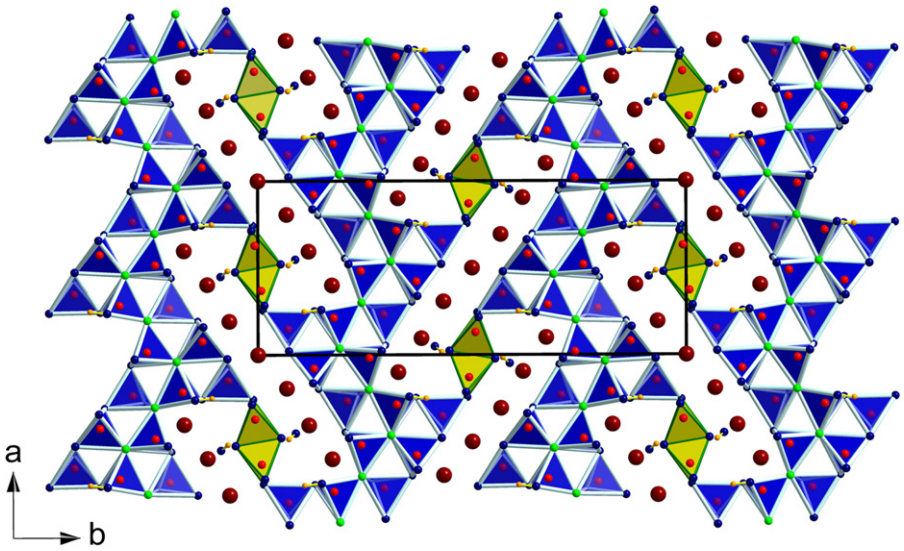

Fig. 1. Crystal structure of $Co_7B_{24}O_{42}(OH)_2 \cdot 2\,H_2O$ along [001], exhibiting corrugated layers of corner-sharing BO_4 tetrahedra. The layers are linked *via* two edge-sharing BO_4 tetrahedra (B_2O_6 unit). Two-fold coordinated oxygen atoms: dark corners of polyhedra and small dark spheres, three-fold coordinated oxygen atoms: light corners of polyhedra, H: light small spheres, B: center of polyhedra, Co: large spheres, light polyhedra: B_2O_6 unit.

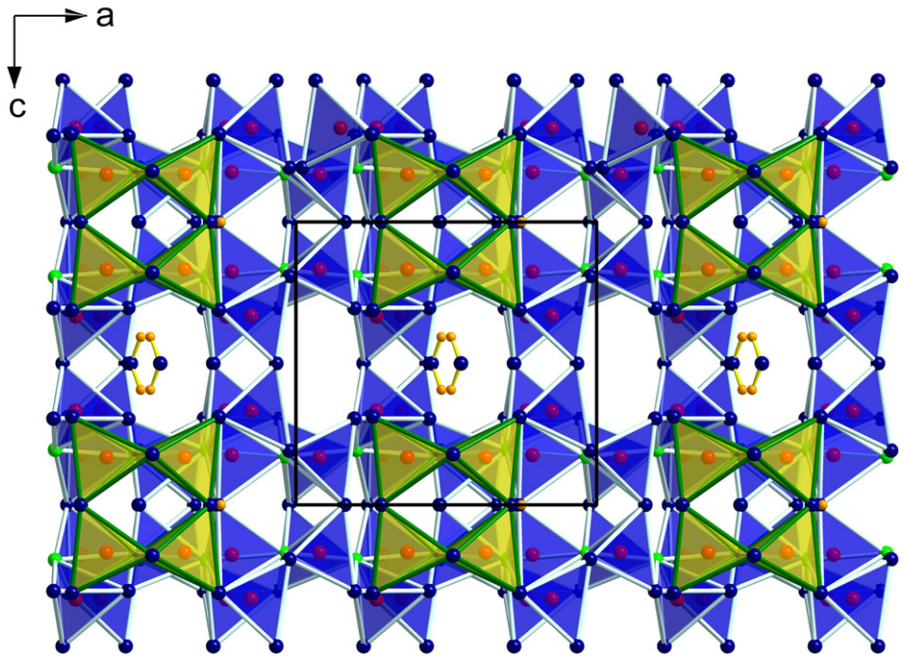

Fig. 2. Crystal structure of $Co_7B_{24}O_{42}(OH)_2 \cdot 2\,H_2O$ along[$0\bar{1}0$], exhibiting "vierer" rings of two corner-sharing B_2O_6 units (light polyhedra). Two-fold coordinated oxygen atoms: dark corners of polyhedra and small dark spheres, three-fold coordinated oxygen atoms: light corners of polyhedra, H: light small spheres, B: center of polyhedra, Co: not depicted.

enlarged B···B distance of 221.5(1) pm. In $Co_7B_{24}O_{42}(OH)_2 \cdot 2\,H_2O$, the large B···B distance is presumably caused by the exceptional linkage of two B_2O_6 groups forming a "vierer" ring (see Figs. 2 and 3).

In $Co_7B_{24}O_{42}(OH)_2 \cdot 2\,H_2O$, three of the four crystallographically independent metal ions are coordinated octahedrally by six oxygen atoms (Co1, Co2, Co4). The other one is surrounded by four oxygen atoms in a distorted tetrahedral way (Co3). The coordination spheres are depicted in Fig. 5. The bond-lengths of the six-fold coordinated cations vary from 207.3 to 235.3 pm with an average value of 214.1 pm. This value is in agreement with the average Co^{2+}–O distance of six-fold coordinated cobalt atoms of 212.2 pm, found in $Co_2B_2O_5$ [31,32]. In the tetrahedral coordination polyhedra, the Co–O distances range from 196.9 to 199.9 pm with a mean value of 199.2 pm. This is slightly lower than the average Co–O distances of 202.7 pm in CoB_4O_7 [31] and agrees with the average value of 198.4 pm in $Co_4(BO_2)_6O$ [31], which both reveal Co^{2+} in four-fold coordination.

Due to a heavy transition metal cation (Co^{2+}), a direct localization of the hydrogen atoms on the basis of the Fourier difference map was difficult. Nevertheless, from bond valence calculations and geometrical reasons the positions of the hydrogen atoms were derived at the oxygen atoms O9, forming water molecules, and O13, forming hydroxyl groups. Fig. 6 gives a view of the position of the hydrogen atoms, which could be refined at the oxygen atoms O9 and O13 without any restraints. In the absence of hydrogen atoms, these oxygen atoms show a significantly reduced value in the bond-length/bond-strength calculation. In fact, the oxygen atom O9 is the only one, which shows no bonds to boron atoms, giving a significant

coordinative contribution to Co1 and Co2. Furthermore, hydrogen bonding can be assumed between the H-atoms and the adjacent O-atoms (see Fig. 6). In the case of H1 (bond to O9, Fig. 6 top), the next O^{2-} ion is O2 with a distance of 179 pm (H1⋯O2). The distances to the oxygen ions O6 and O2 show values of 254 and 307 pm, respectively. The hydrogen bonds of H2 (bond to O13, Fig. 6 bottom) reveal values of 191 pm for H2⋯O14, 249 pm for H2⋯O1, and 308 pm for the distance H2⋯O6. Comparable distances of hydrogen bonds can be found in $Co(OH)_2$ (245(6) pm) [33] and $Co_6B_{22}O_{39}\cdot H_2O$ (245 and 304 pm) [17].

Interestingly, this structure is akin to the structure of $M_6B_{22}O_{39}\cdot H_2O$ (M=Fe, Co), which exhibits intermediate states on the way to edge-sharing BO_4 tetrahedra. The compound is built up from corrugated multiple layers of corner-sharing BO_4 groups, which are interconnected by BO_3 units. The connecting BO_3 groups are distorted and close to BO_4 tetrahedra, if additional oxygen atoms of the neighboring BO_4 tetrahedra are considered in the coordination sphere. This situation may be regarded as an intermediate state in the formation of edge-sharing tetrahedra. A comparison of $M_6B_{22}O_{39}\cdot H_2O$ (M=Fe, Co) and $Co_7B_{24}O_{42}(OH)_2\cdot 2\,H_2O$ is given in Fig. 7. Both compounds were synthesized

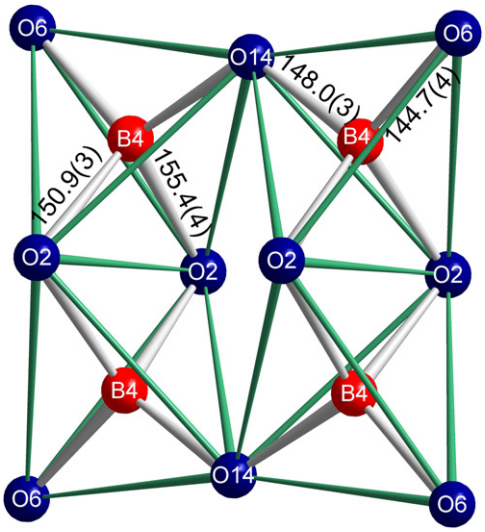

Fig. 3. "Vierer" ring of two corner-sharing B_2O_6 units with bond distances in pm. A new structural motive in the chemistry of borates.

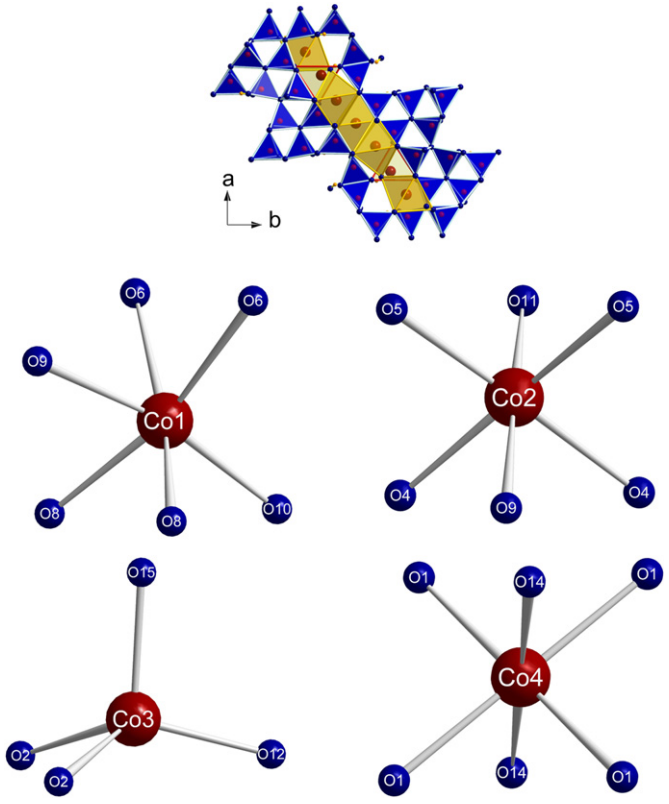

Fig. 5. Coordination spheres of Co^{2+} ions in $Co_7B_{24}O_{42}(OH)_2\cdot 2\,H_2O$. Top: Octahedral coordination spheres of Co1, Co2, and Co4 in $Co_7B_{24}O_{42}(OH)_2\cdot 2\,H_2O$: light polyhedra with light corners, tetrahedral coordination spheres of Co3: light polyhedra with dark corners.

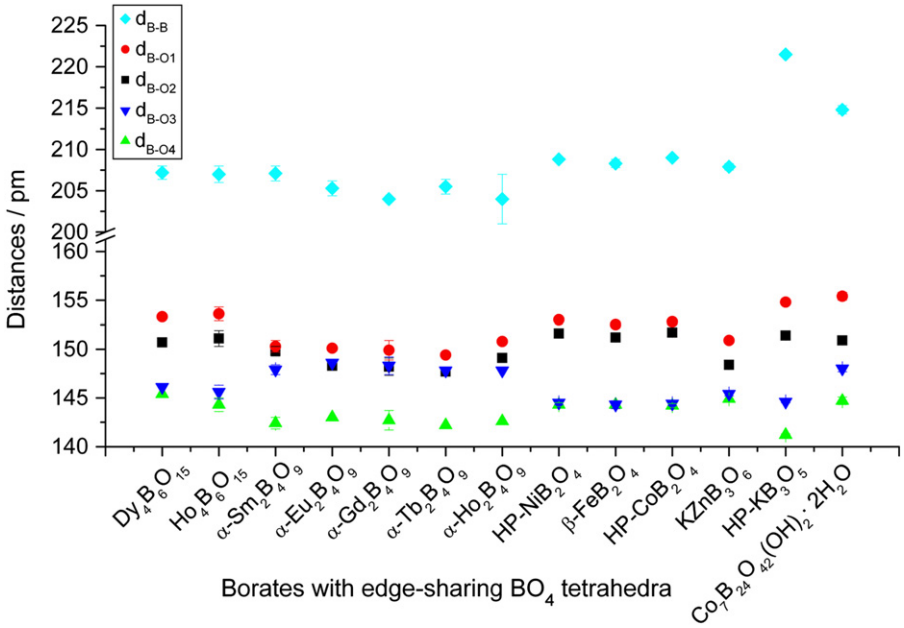

Fig. 4. Comparison of the interatomic distances inside the edge-sharing BO_4 tetrahedra of all currently known compounds; d_{B-B} is the interatomic distance of the two boron atoms inside the B_2O_2 ring, d_{B-O1} and d_{B-O2} represent the B–O distances inside the B_2O_2 ring, d_{B-O3} and d_{B-O4} are those outside the ring.

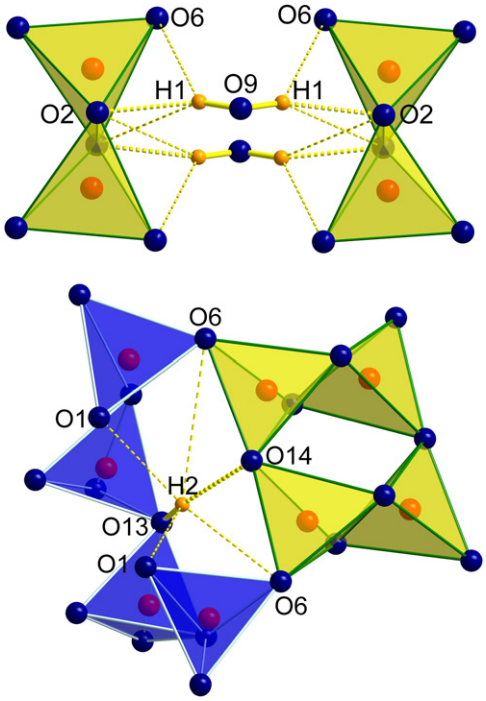

Fig. 6. Position of the hydrogen-atoms in $Co_7B_{24}O_{42}(OH)_2 \cdot 2\,H_2O$; top: position of H1, bottom: position of H2. Oxygen atoms: dark corners of polyhedra and small spheres, B: center of polyhedra, and H: light sphere; dashed lines represent hydrogen bridges.

at the same pressure (6 GPa) and similar temperatures ($Co_7B_{24}O_{42}(OH)_2 \cdot 2\,H_2O$: 880 °C, $Co_6B_{22}O_{39} \cdot 2\,H_2O$: 950 °C). Because at lower temperatures less water is expelled from the sample, the slightly lower temperatures for the synthesis of $Co_7B_{24}O_{42}(OH)_2 \cdot 2\,H_2O$ lead to a higher water content in the structure.

Additionally, the bond valence sums for all atoms of $Co_7B_{24}O_{42}(OH)_2 \cdot 2\,H_2O$ were calculated, using the bond-length/bond-strength (ΣV) [34,35] and the CHARDI concept (*charge distribution* in solids, ΣQ) [36] (Table 4). The formal ionic charges of the atoms are consistent within the limits of the concept, except for O9, O13, and O14, which participate in the hydrogen bonds. Due to the free refinement of the hydrogen atoms, the O–H distances appear to be shorter than they actually are (O9-H1: 84(4) pm; O13-H2: 79(7) pm). Thus, the calculated valence sums are increased for atoms, that are covalently bond to hydrogen (O9, O13) and decreased for hydrogen bond acceptors (O14).

The MAPLE-values (*ma*delung *p*art of *l*attice *e*nergy) [37–39] were calculated in order to compare the results with the MAPLE-values, received from CoO [40], H_2O (hexagonal ice) [41], and the high-pressure modification B_2O_3-II [42]. This can be managed by the additive potential of the MAPLE-values, which allows to calculate hypothetical values for $Co_7B_{24}O_{42}(OH)_2 \cdot 2\,H_2O$, starting from the binary oxides. As a result, we obtained a value of 312257 kJ/mol for $Co_7B_{24}O_{42}(OH)_2 \cdot 2\,H_2O$ to be compared with 310227 kJ/mol (deviation 0.7%), starting from the binary oxides (7 CoO (4560 kJ/mol) [40] + 3 H_2O (5017 kJ/mol) [41] + 12 B_2O_3-II (21938 kJ/mol) [42]).

3.2. FTIR spectroscopy

In Fig. 8 the FTIR spectrum of $Co_7B_{24}O_{42}(OH)_2 \cdot 2\,H_2O$ is displayed. The wavenumbers of absorption bands are given in Table 5. Bands around 700 cm^{-1} are typical for bending vibrations of BO_4 groups [43–45]. Between 800 cm^{-1} and 1100 cm^{-1}, stretching vibrations of tetrahedrally coordinated boron atoms are expected. The bands in the range of 1200–1450 cm^{-1} are normally assigned to stretching vibrations of BO_3 groups [46–49]. As $Co_7B_{24}O_{42}(OH)_2 \cdot 2\,H_2O$ does not contain BO_3 groups, the bands in this region are presumably due to OB_3 or B_2O_6 units, which also show stretching vibrations in this wavenumber range [16,17]. Bands from 1600 to 1800 cm^{-1} and from 3100 to 3800 cm^{-1} can be assigned to bending and stretching vibrations of hydroxyl groups and H_2O molecules.

3.3. Raman spectroscopy

The Raman spectrum and the corresponding wavenumbers of bands of a $Co_7B_{24}O_{42}(OH)_2 \cdot 2\,H_2O$ single crystal are displayed in Fig. 9 and Table 6, respectively. Due to strong light absorption of the crystal, the spectrum was acquired at low laser power, resulting in a rather low signal-to-noise ratio of bands at higher wavenumbers. In total, 27 bands in the range of 100–1600 cm^{-1} could be detected. In contrast to FTIR, no bands were observed between 3000 cm^{-1} and 4000 cm^{-1}, which is probably related to the mentioned light absorption problems.

The Raman spectrum of $Co_7B_{24}O_{42}(OH)_2 \cdot 2\,H_2O$ shows five intense bands at and below 300 cm^{-1} and one intense, split band around 550 cm^{-1}. Several bands of medium to low intensity occur between 330-670 cm^{-1}, followed by broad and weak bands at approximately 850, 1030, 1200, 1310, 1450, and 1530 cm^{-1}. Generally, bands below 800 cm^{-1} in borates are assigned to bending vibrations of the BO_4 tetrahedra, vibrations related to cation–oxygen bonds, and complex lattice vibrations.

In the range from 800 to 1100 cm^{-1}, stretching vibrations of BO_4 tetrahedra are expected, whereas above 1100 cm^{-1} Raman modes are related to BO_3 and OB_3 ($O^{[3]}$) groups as well as edge-sharing BO_4 tetrahedra ($[B_2O_6]^{6-}$). The latter were previously investigated by comparative studies of Raman-active modes of edge-sharing BO_4 tetrahedra, which were performed on HP-NiB_2O_4 [12], α-$Gd_2B_4O_9$ [9], $Dy_4B_6O_{15}$ [7], and $Co_6B_{22}O_{39} \cdot H_2O$ [17]. The spectra of these compounds reveal several bands in the range of 1200–1450 cm^{-1}, which do not correspond to BO_3 or OB_3 groups. This leads to two bands, that most probably can be assigned to modes of edge-sharing BO_4 tetrahedra (B_2O_6 unit) (1262 and 1444 cm^{-1} in HP-NiB_2O_4, 1253 and 1431 cm^{-1} in α-$Gd_2B_4O_9$, 1271 and 1435 cm^{-1} in $Dy_4B_6O_{15}$, and 1180 and 1450 cm^{-1} in $Co_6B_{22}O_{39} \cdot H_2O$). Therefore, the bands at 1198 and 1447 cm^{-1} in the Raman spectrum of $Co_7B_{24}O_{42}(OH)_2 \cdot 2\,H_2O$ are most probably caused by vibrational modes of the B_2O_6 unit. Jin et al. also found an absorption in the range of 1400 cm^{-1} for the recently published $KZnB_3O_6$ [15], but eventually missed a weak B_2O_6 vibration at 1210 cm^{-1}.

Recent DFT calculations [50] of vibrational modes of HP-KB_3O_5 allowed for the first time a precise assignment of previously discussed vibrational modes of these B_2O_6 groups. The compound HP-KB_3O_5 exhibits a band at 1213 cm^{-1}, caused by strong vibrations within the B_2O_6 unit but no band around 1400 cm^{-1}, which is caused by vibrations of the B_2O_6 unit. This difference to other compounds comprising edge-sharing BO_4 tetrahedra might be due to the exceptionally increased boron coordination of the oxygen atoms within the common edge of the two edge-sharing BO_4 tetrahedra in HP-KB_3O_5. As $Co_7B_{24}O_{42}(OH)_2 \cdot 2\,H_2O$ does not contain BO_3 groups, the bands between 1200 and 1530 cm^{-1} are most probably vibrational modes of the $[B_2O_6]^{6-}$ (1198 and 1447 cm^{-1}) and the OB_3 units.

4. Conclusions

The new cobalt borate hydrate $Co_7B_{24}O_{42}(OH)_2 \cdot 2\,H_2O$ is built up from corrugated layers of corner-sharing BO_4 tetrahedra, which are interconnected to a three dimensional network by a $[B_2O_6]^{6-}$ unit (two edge-sharing BO_4 tetrahedra). The new compound is closely related to $M_6B_{22}O_{39} \cdot H_2O$ (M=Fe, Co) [17], which exhibits a structural feature, that can be considered as an

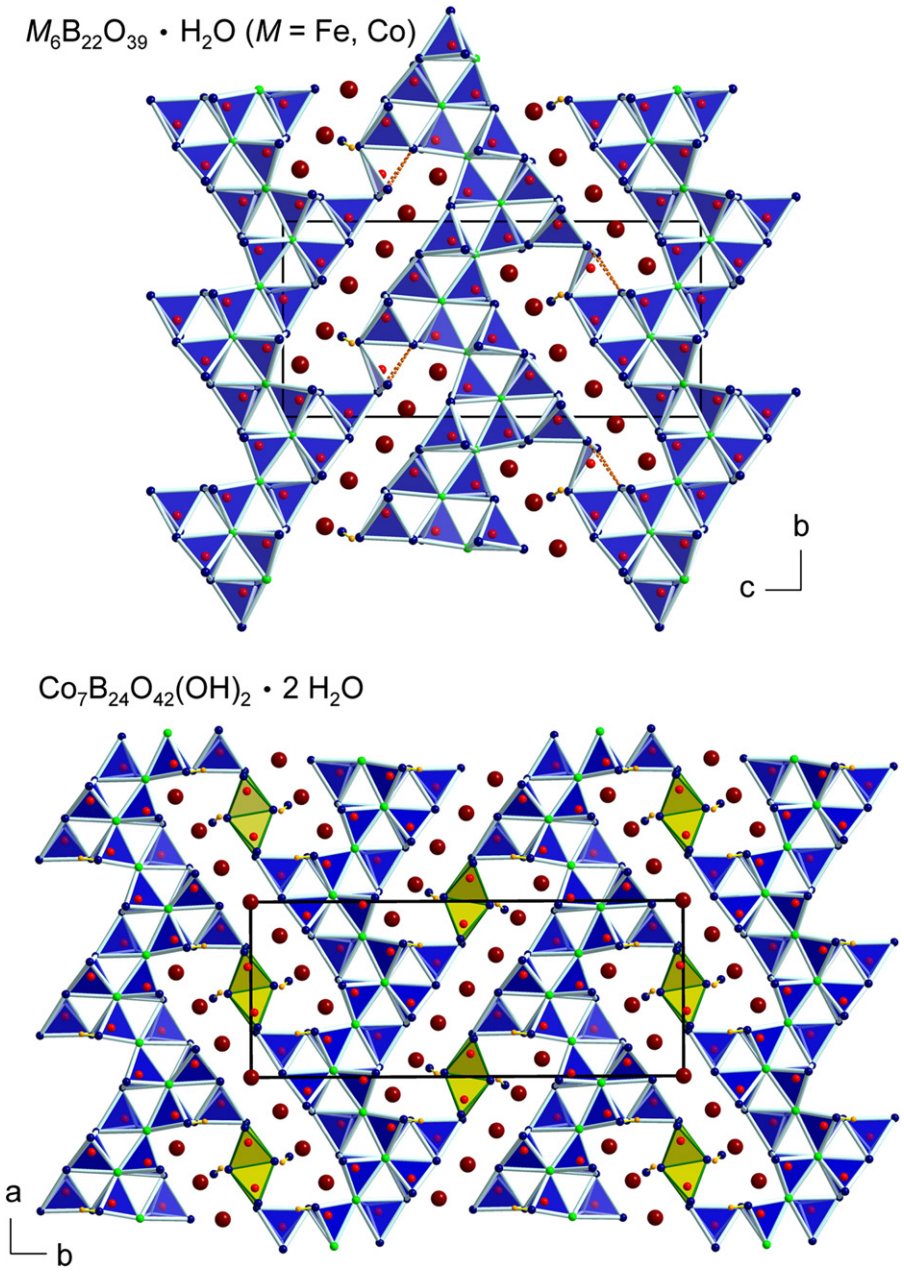

Fig. 7. Comparison of the crystal structures of $M_6B_{22}O_{39} \cdot H_2O$ (M=Fe, Co) (top) and $Co_7B_{24}O_{42}(OH)_2 \cdot 2\ H_2O$ (bottom). Two-fold coordinated oxygen atoms: dark corners of polyhedra and small dark spheres, three-fold coordinated oxygen atoms: light corners of polyhedra, H: light small spheres, B: center of polyhedra, Co: large spheres, light polyhedra: B_2O_6 unit.

Table 4
Charge distribution in $Co_7B_{24}O_{42}(OH)_2 \cdot 2\ H_2O$, calculated with the bond-length/bond-strength ($\sum$V) and the Chardi ($\sum$Q) concept.

	Co1	Co 2	Co 3	Co 4		B1	B2	B3	B4	B5	B6
$\sum$V	+1.69	+2.05	+1.77	+1.72		+2.98	+3.04	+2.96	+2.86	+3.07	+3.12
$\sum$Q	+1.90	+1.90	+2.08	+2.07		+3.02	+3.04	+3.00	+3.28	+2.97	+3.01
	O1	O2	O3	O4	O5	O6	O7	O8	O9	O10	O11
$\sum$V	−1.88	−1.85	−2.16	−2.01	−1.96	−1.81	−1.96	−1.93	−3.32	−1.89	−1.96
$\sum$Q	−1.97	−1.78	−2.03	−2.05	−1.98	−1.97	−1.74	−2.05	−2.65	−2.03	−2.07
	O12	O13	O14	O15							
$\sum$V	−2.09	−2.85	−1.66	−2.00							
$\sum$Q	−2.13	−2.19	−1.77	−2.03							

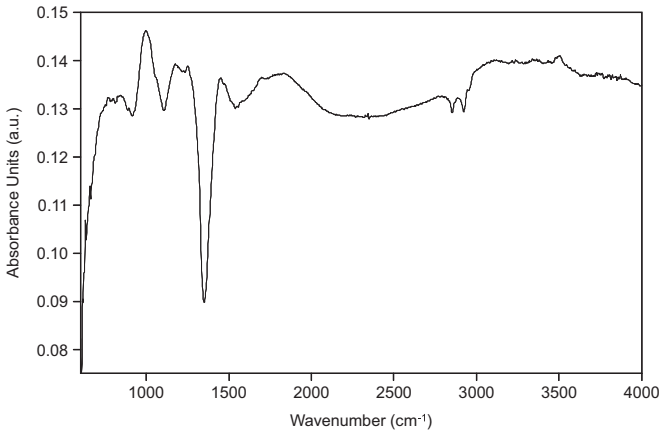

Fig. 8. FTIR absorbance spectrum of a $Co_7B_{24}O_{42}(OH)_2 \cdot 2\,H_2O$ single crystal in the range of 600–4000 cm^{-1}.

Table 5
Wavenumbers (cm^{-1}) and possible assignment of FTIR–absorption bands in the spectrum of $Co_7B_{24}O_{42}(OH)_2 \cdot 2\,H_2O$.

Band	Assignment
642	$\delta(BO_4)$
716	
835	$\nu(BO_4)$
1006	
1184	$\nu(BO_4)$
1267	
1308	$\nu(OB_3)$
1433	$\nu(B_2O_6)$
1511	
1645	$\delta(OH)$
1803	
3104	$\nu(OH)$
3240	
3363	
3435	
3499	
3797	

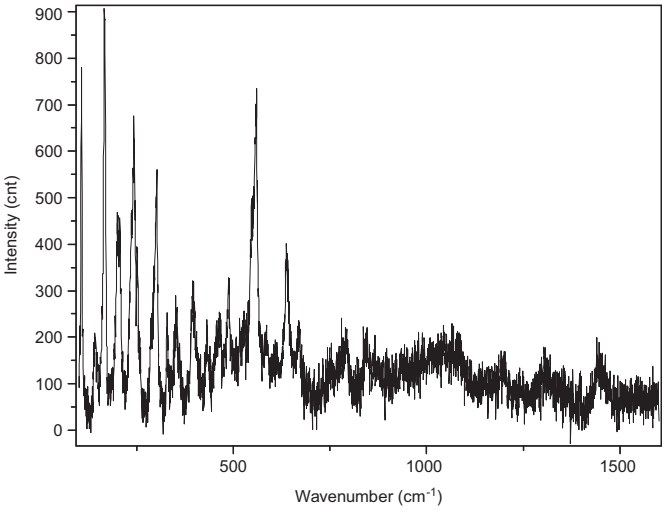

Fig. 9. Raman spectrum of a $Co_7B_{24}O_{42}(OH)_2 \cdot 2\,H_2O$ single crystal in the range of 100–1600 cm^{-1}.

Table 6
Wavenumbers (cm^{-1}) and possible assignment of Raman bands in the spectrum of $Co_7B_{24}O_{42}(OH)_2 \cdot 2\,H_2O$.

Band	Assignment
107	Lattice Co–O
143	
163	
167	
200	
207	
242	
252	
291	
301	
329	
353	
396	
432	Bending (BO_4)
461	
487	
546	
549	
559	
638	
669	
771	Stretching (BO_4)
781	
850	
1030	
1198	Stretching (B_2O_6) and (OB_3)
1311	
1447	
1532	

intermediate state on the way to edge-sharing BO_4 tetrahedra. Further investigations in borates under enhanced pressure conditions will certainly lead to many new borates possessing the structural motive of edge-sharing BO_4 tetrahedra. Together with the results obtained so far, these prospective findings might provide new insights into the reaction path and the general occurrence of edge-sharing BO_4 tetrahedra in the structural chemistry of borates. Due to the fact that five of six structure types with edge-sharing BO_4 tetrahedra were synthesized under high-pressure conditions and that another compound reveals an intermediate state ($M_6B_{22}O_{39} \cdot H_2O$ (M=Fe, Co)), we can clearly formulate: pressure favours the formation of edge-sharing BO_4 tetrahedra in the chemistry of borates.

Acknowledgments

We gratefully acknowledge the continuous support by Prof. W. Schnick, Department of Chemistry of the University of Munich (LMU). Special thanks go to Dr. J. Knyrim for synthesizing the crystal and M. Glätzle for optimizing the synthesis. We also thank Dr. G. Heymann for collecting the single-crystal data.

Appendix A. Supplementary materials

Supplementary materials associated with this article can be found in the online version at doi:10.1016/j.jssc.2011.10.028.

References

[1] H. Huppertz, Z. Kristallogr. 219 (2004) 330.

[2] J.S. Knyrim, P. Becker, D. Johrendt, H. Huppertz, Angew. Chem. 118 (2006) 8419;
J.S. Knyrim, P. Becker, D. Johrendt, H. Huppertz, Angew. Chem. Int. Ed. 45 (2006) 8239.
[3] J.S. Knyrim, F.M. Schappacher, R. Pöttgen, J. Schmedt auf der Günne, D. Johrendt, H. Huppertz, Chem. Mater. 19 (2007) 254.
[4] S.C. Neumair, H. Huppertz, Z. Naturforsch. 64B (2009) 1339.
[5] H. Emme, M. Valldor, R. Pöttgen, H. Huppertz, Chem. Mater. 17 (2005) 2707.
[6] H. Huppertz, B. von der Eltz, J. Am. Chem. Soc. 124 (2002) 9376.
[7] H. Huppertz, Z. Naturforsch. 58B (2003) 278.
[8] H. Emme, H. Huppertz, Z. Anorg. Allg. Chem. 628 (2002) 2165.
[9] H. Emme, H. Huppertz, Chem. Eur. J. 9 (2003) 3623.
[10] H. Emme, H. Huppertz, Acta Crystallogr. Sect. 61C (2005) i29.
[11] S.C. Neumair, R. Kaindl, H. Huppertz, Z. Naturforsch. 65B (2010) 1311.
[12] J.S. Knyrim, F. Roeßner, S. Jakob, D. Johrendt, I. Kinski, R. Glaum, H. Huppertz, Angew. Chem. 119 (2007) 9256;
J.S. Knyrim, F. Roeßner, S. Jakob, D. Johrendt, I. Kinski, R. Glaum, H. Huppertz, Angew. Chem. Int. Ed. 46 (2007) 9097.
[13] S.C. Neumair, R. Glaum, H. Huppertz, Z. Naturforsch. 64B (2009) 883.
[14] Y. Wu, J.-Y. Yao, J.-X. Zhang, P.-Z. Fu, Y.-C. Wu, Acta Crystallogr. Sect. 66E (2010) i45.
[15] S. Jin, G. Cai, W. Wang, M. He, S. Wang, X. Chen, Angew. Chem. 122 (2010) 5087;
S. Jin, G. Cai, W. Wang, M. He, S. Wang, X. Chen, Angew. Chem. Int. Ed. 49 (2010) 4967.
[16] S.C. Neumair, S. Vanicek, R. Kaindl, D. Többens, C. Martineau, F. Taulelle, J. Senker, H. Huppertz, Eur. J. Inorg. Chem. 2011 (2011) 4147.
[17] S.C. Neumair, J.S. Knyrim, O. Oeckler, R. Glaum, R. Kaindl, R. Stalder, H. Huppertz, Chem. Eur. J. 16 (2010) 13659.
[18] D. Walker, M.A. Carpenter, C.M. Hitch, Am. Miner. 75 (1990) 1020.
[19] D. Walker, Am. Miner. 76 (1991) 1092.
[20] D.C. Rubie, Phase Trans. 68 (1999) 431.
[21] N. Kawai, S. Endo, Rev. Sci. Instrum. 41 (1970) 1178.
[22] Treor90, P.-E. Werner, University of Stockholm, 1990.
[23] P.-E. Werner, Z. Kristallogr, Kristallgeom. Kristallphys. Kristallchem. 120 (1964) 375.
[24] P.-E. Werner, L. Errikson, M. Westdahl, J. Appl. Crystallogr. 18 (1985) 367.
[25] Z. Otwinowski, W. Minor, Methods Enzymol. 276 (1997) 307.
[26] G.M. Sheldrick, SHELXL-97 and SHELXS-97, Program Suite for the Solution and Refinement of Crystal Structures, University of Göttingen, Göttingen, Germany, 1997.
[27] G.M. Sheldrick, Acta Crystallogr. Sect. A64 (2008) 112.
[28] The term "vierer" ring was coined by F. Liebau (Structural Chemistry of Silicates, Springer, Berlin, 1985) and is derived from the german word "vier", which means four. However, a "vierer" ring is not a four membered ring, but rather a ring with four tetrahedral centers (B). Similar terms exist for rings made up of two or three tetrahedral centers, namely "zweier" and "dreier" rings.
[29] E. Zobetz, Z. Kristallogr. 191 (1990) 45.
[30] F.C. Hawthorne, P.C. Burns, J.D. Grice, in: E.S. Grew (Ed.), Boron: Mineralogy, Petrology and Geochemistry, Mineralogical Society of America, Washington, 1996.
[31] J.L.C. Rowsell, N.J. Taylor, L.F. Nazar, J. Solid State Chem. 174 (2003) 189.
[32] S.V. Berger, Acta Chem. Scand. 4 (1950) 1054.
[33] F. Pertlik, Monatsh. Chem. 130 (1999) 1083.
[34] I.D. Brown, D. Altermatt, Acta Crystallogr. Sect. 41B (1985) 244.
[35] N.E. Brese, M. O'Keeffe, Acta Crystallogr. Sect. 47B (1991) 192.
[36] R. Hoppe, S. Voigt, H. Glaum, J. Kissel, H.P. Müller, K.J. Bernet, J. Less-Common Met. 156 (1989) 105.
[37] R. Hoppe, Angew. Chem. 78 (1966) 52;
R. Hoppe, Angew. Chem. Int. Ed. 5 (1966) 95.
[38] R. Hoppe, Angew. Chem. 82 (1970) 7;
R. Hoppe, Angew. Chem. Int. Ed. 9 (1970) 25.
[39] R. Hübenthal, MAPLE—Program for the Calculation of Maple Values (Vers. 4) University of Giessen, Giessen, Germany, 1993.
[40] N.C. Tombs, H.P. Rooksby, Nature 165 (1950) 442.
[41] A. Goto, T. Hondoh, S. Mae, J. Chem. Phys. 93 (1990) 1412.
[42] C.T. Prewitt, R.D. Shannon, Acta Crystallogr. Sect. 24B (1968) 869.
[43] J.P. Laperches, P. Tarte, Spectrochim. Acta 22 (1966) 1201.
[44] G. Heymann, K. Beyer, H. Huppertz, Z. Naturforsch. B59 (2004) 1200.
[45] C.E. Weir, R.A. Schroeder, J. Res., Nat. Bur. Stands 68A (1964) 465.
[46] S.D. Ross, Spectrochim. Acta A 28 (1972) 1555.
[47] W.C. Steele, J.C. Decius, J. Chem. Phys. 25 (1956) 1184.
[48] R. Böhlhoff, H.U. Bambauer, W. Hoffmann, Z. Kristallogr. 133 (1971) 386.
[49] K. Machida, H. Hata, K. Okuno, G. Adachi, J. Shiokawa, J. Inorg. Nucl. Chem. 41 (1979) 1425.
[50] Vibrational frequencies were computed from first principles, using the program CRYSTAL 06 (R. Dovesi, V.R. Saunders, C. Roetti, R. Orlando, C. M. Zicovich-Wilson, F. Pascale, B. Civalleri, K. Doll, N.M. Harrison, I.J. Bush, Ph. D'Arco, M. Llunell, CRYSTAL06—User's Manual, University of Torino, Torino, 2006, Gaussian basis sets, and the B3LYP Hybrid HF-DFT functional.